Monthly Notices
of the
ROYAL ASTRONOMICAL SOCIETY

MNRAS **464,** 2698–2707 (2017)
Advance Access publication 2016 September 23

doi:10.1093/mnras/stw2422

Optimal redshift weighting for redshift-space distortions

Rossana Ruggeri,[1⋆] Will J. Percival,[1⋆] Héctor Gil-Marín,[1,2,3] Fangzhou Zhu,[4] Gong-Bo Zhao[1,5] and Yuting Wang[1,5]

[1]*Institute of Cosmology and Gravitation, University of Portsmouth, Dennis Sciama Building, Portsmouth PO1 3FX, UK*
[2]*Sorbonne Université, Institut Lagrange de Paris (ILP), 98 bis Boulevard Arago, F-75014 Paris, France*
[3]*Laboratoire de Physique Nucléaire et de Hautes Energies, Université Pierre et Marie Curie, F-75252 Paris cedex 05, France*
[4]*Department of Physics, Yale University, New Haven, CT 06511, USA*
[5]*National Astronomy Observatories, Chinese Academy of Science, Beijing 100012, P.R.China*

Accepted 2016 September 22. Received 2016 September 20; in original form 2016 February 16

ABSTRACT

The low-statistical errors on cosmological parameters promised by future galaxy surveys will only be realized with the development of new, fast, analysis methods that reduce potential systematic problems to low levels. We present an efficient method for measuring the evolution of the growth of structure using redshift-space distortions (RSDs), that removes the need to make measurements in redshift shells. We provide sets of galaxy-weights that cover a wide range in redshift, but are optimized to provide differential information about cosmological evolution. These are derived to optimally measure the coefficients of a parametrization of the redshift-dependent matter density, which provides a framework to measure deviations from the concordance ΛCDM cosmology, allowing for deviations in both geometric and/or growth. We test the robustness of the weights by comparing with alternative schemes and investigate the impact of galaxy bias. We extend the results to measure the combined anisotropic baryon acoustic oscillation and RSD signals.

Key words: surveys – galaxies: statistics – cosmological parameters – cosmology: observations – large-scale structure of Universe.

1 INTRODUCTION

Forthcoming galaxy redshift surveys are motivated, to a large extent, by obtaining galaxy clustering measurements to accurately quantify the observed acceleration in the expansion of the Universe. It is to be hoped that these observations will reveal insight into the physical mechanism responsible for the cosmic acceleration, be it a new scalar field currently contributing to the energy budget of the Universe as dark energy, modification of gravitational laws on cosmological scales, or an unknown alternative to the standard cosmological model.

Because the large-scale galaxy distribution is expected to follow a Gaussian random field, the statistical information is fully encoded in 2-point statistics, the central quantities in the analysis of galaxy surveys are the correlation function and its Fourier-space analogue, the power spectrum. The observed projections of these quantities encode significant cosmological information, including the positions of the baryonic acoustic oscillations (BAOs), which can be used as standard rulers to reconstruct the expansion history of the Universe (Gil-Marín et al. 2016). The statistics also encode redshift space distortions (RSDs) that provide information about the large-scale growth of cosmological structure (Hamilton 1998).

The improvement in the statistical precision afforded by forthcoming surveys including DESI (Levi et al. 2013) and Euclid (Laureijs et al. 2011) is impressive, and will push at least an order of magnitude beyond current measurements. The improvement warrants a concerted effort to improve the methods used to analyse these data, and recent key developments include 'reconstruction' to remove nonlinear BAO damping (Eisenstein, Seo & White 2007), and the development of fast methods to measure the anisotropic clustering signal (Bianchi et al. 2015; Scoccimarro 2015).

One additional question to be answered is how best to combine future data from different volumes within the surveys, without losing information from galaxy pairs that span different bins, if using a binned approach and to optimally recover the desired signal. To deal with the first concern, we can make the transition from splitting into redshift-bins, to instead adopting weights that act to provide smoother windows on the data.

To optimize the weights, we must consider two factors: the first concerns changes in the observational efficiency as a function of position on the sky and redshift, and leads to weights that vary as a function of observed galaxy density (Feldman, Kaiser & Peacock 1994) and bias (Percival, Verde & Peacock 2004). The second concerns the cosmological models that we wish to distinguish between:

⋆ E-mail: rossana.ruggeri@port.ac.uk (RR); will.percival@port.ac.uk (WJP)

Feldman et al. (1994) and Percival et al. (2004) wished to optimally measure a power spectrum that was assumed to be fixed within a survey volume. If instead, we wish to measure cosmological parameters that vary across a sample, for example a quantity that evolves with redshift, then the weights must additionally be optimized to measure this evolution.

In general, RSD measurements are made for a particular volume, presented as a single measurement at an effective redshift; if e.g. the growth factor varies in a non-linear way across the sample, the effective redshift is not a good approximation, by contrast by weighting the sample we allow for variation in redshift of all the measured quantities.

Zhu, Padmanabhan & White (2015) presented weights optimized for measuring the distance–redshift relationship using the BAO signal. They considered a second-order expansion of the distance–redshift relationship around a fiducial cosmological model, and provided sets of weights for the monopole and quadrupole moments of the correlation function (or power spectrum) designed to optimally measure these parameters. In this paper, we extend this derivation to the measurement of RSDs, considering the weights required for these measurements, and how they compare to the BAO-optimized weights.

The outline of the paper is as follows. In Section 2, we briefly go through the method of linear data compression and we underline the advantages related. In Section 3, we present the cosmological model. In Section 4, we build to a derivation of the optimal weighting scheme for RSD measurements parametrized with respect to the matter energy density evolution in redshift, $\Omega_{\rm m}(z)$. The choice of $\Omega_{\rm m}$ parametrization allows us to easily extend the results for more general clustering models that include both RSD and Alcock & Paczyński (AP) effects (1979). In the second part of the section we compare them with other possible weights optimized for RSD measurements and we discuss our assumption for linear bias model. In Section 5, we derive the generalization of optimal weights for RSD and AP test combined measurements. In Section 6, we discuss our results and present potential future improvements and applications.

2 OPTIMAL WEIGHTS

The derivation of optimal weights is equivalent to the problem of optimal data compression: we use the weights to reduce the number of data points that need to be analysed to recover the cosmological parameters. We will now review how to optimally linearly compress our data, in the case of a covariance matrix known a priori, as described in Tegmark, Taylor & Heavens (1997). Further details on the Karhunen–Loève methods in e.g. Vogeley & Szalay (1996) and Pope et al. (2004).

Given the n-dimensional data set $\boldsymbol{x}$, assumed to be Gaussian distributed with mean $\boldsymbol{\mu}$ and covariance C, it can be linearly compressed into a new data set y,

$$y = \boldsymbol{w}^{\rm T}\boldsymbol{x}, \tag{1}$$

where $\boldsymbol{w}$ is a n-dimensional vector of weights. The measurement y has mean $\boldsymbol{w}^{\rm T}\mu$ and variance $\boldsymbol{w}^{\rm T}C\boldsymbol{w}$.

The Fisher information matrix $\mathbf{F}$ is defined as the second derivative of the logarithmic likelihood function $\mathcal{L} \equiv -\ln L$,

$$\mathbf{F}_{ij} \equiv \left\langle \frac{\partial^2 \mathcal{L}}{\partial\theta_i \partial\theta_j} \right\rangle, \tag{2}$$

for a set of parameters to be measured θ_i. For a single parameter θ_i,

$$\mathbf{F}_{ii} = \frac{1}{2}\left(\frac{\boldsymbol{w}^{\rm T}C_{,i}\boldsymbol{w}}{\boldsymbol{w}^{\rm T}C\boldsymbol{w}}\right)^2 + \frac{\left(\boldsymbol{w}^{\rm T}\mu_{,i}\right)^2}{\boldsymbol{w}^{\rm T}C\boldsymbol{w}}, \tag{3}$$

where the index, i, denotes $\partial/\partial\theta_i$. Note that the normalization of the weights is arbitrary. The search for optimal weights is equivalent to maximizing $\mathbf{F}_{ii}$ with respect to $\boldsymbol{w}$.

For a measurement of 2-point statistics from a galaxy survey, we should consider that $\boldsymbol{x}$ is the arrays formed by the measurements of the overdensity squared, δ^2 in configuration or the Fourier space. Working in the Fourier space, the covariance matrix $\mathbf{C}$ of the power spectrum of the modes in the absence of a survey window is diagonal; for each redshift slice with volume dV and expected galaxy density $\overline{n}(r)$,

$$C \sim (P_{\rm fid} + 1/\overline{n}(r))^2 \frac{1}{{\rm d}V}, \tag{4}$$

where we have made the assumption that around the likelihood maxima, the power spectra P_{fid} are drawn from a Gaussian distribution with fixed covariance matrix, e.g. Kalus, Percival & Samushia (2016). In this case, the first term in equation (3) vanishes. Maximizing $\mathbf{F}_{ii}$ with respect to $\boldsymbol{w}$, we find the only non-trivial eigenvector to be

$$\boldsymbol{w}^{\rm T} = \mathbf{C}^{-1}\mu_{,i}, \tag{5}$$

and the new compressed data set reduces to

$$y = \mu_{,i}^{\rm T}\mathbf{C}^{-1}\boldsymbol{x}. \tag{6}$$

Note that, to linear order, y contains the same information as $\boldsymbol{x}$, which can be checked by substituting $\boldsymbol{w} = \mathbf{C}^{-1}\mu_{,i}$ in equation (3), and seeing that $\mathbf{F}$ remains unchanged. Equation (5) forms the basis for our derivation of optimal weights.

Equation (3) shows why it does not make sense to optimize the set of δ (as opposed to δ^2). This is because, although the second term in equation (3) now vanishes as $\langle\delta\rangle = 0$, the resulting eigenvector equation derived from the first term shows that there is no single set of optimal weights, even under the simplifying assumption of a diagonal covariance matrix. We can still apply the weights derived for δ^2 to individual galaxies if we assume that the scales upon which clustering is being measured are small with respect to the cosmological changes that affect the relative weights. We would then simply weight each galaxy (and the expected density used to estimate δ) by $\boldsymbol{w}_{\rm gal} = \sqrt{\boldsymbol{w}_{\delta^2}}$.

Note that the optimal set of weights given in equation (5) depends upon the derivatives of $\mu_i = P_{,i}$. Consequently in the rest of the paper we concentrate our analysis on the form of $P_{,i}$, which directly gives the form for the weights. If $P_{,i}$ matches for different measurements, then the optimal weights will also match.

The weights can be seen as a generalization of the Feldman-Kaiser-Peacok (FKP), weights presented in Feldman et al. (1994). The FKP weights are obtained by minimizing the fractional variance in the power under the assumption that fluctuations are Gaussian and have the form

$$w_{\rm FKP}(r) = \frac{1}{1 + \overline{n}(r)P(k)}. \tag{7}$$

The weights defined by equation (5) depend on the inverse of the covariance matrix: assuming the redshift slices to be independent we can invert the covariance matrix for a chosen scale and recover the FKP weights.

The cosmological model dependent weights depend on the covariance matrix assumed and on the derivative of the mean value of

the model with respect to the parameter that we want to estimate. Thus, once these quantities are fixed, it is not trivial to adapt a particular set of weights for different models. However, it would be very useful to set up weights that can be applied to make different measurements: both for computational reasons and in order to perform joint fits to the data. In this work, we will start by deriving weights to be applied to RSD measurements and then we will broaden this to consider jointly measuring the RSD and the AP effect. Comparing the set of weights in these different situations shows whether it is likely that a single set of weights can be used to make optimal measurements in both situations.

3 COSMOLOGICAL MODEL

3.1 Fiducial cosmology

The ΛCDM scenario predicts the nature of dark energy as a cosmological constant with equation-of-state parameter $w = -1$, where the dynamical expansion of the Universe is specified by Friedmann equation

$$\frac{H^2_{\rm fid}(z)}{H^2_{0,\rm fid}} = \Omega_{m,0,\rm fid}(1+z)^3 + \Omega_{k,\rm fid}(1+z)^2 + \Omega_{\Lambda,\rm fid}(z), \tag{8}$$

where the subscript the '0' stands for quantities evaluated at $z = 0$ while 'fid' denotes fiducial quantities. With $\Omega_{\Lambda,\rm fid}$ dark energy density, $\Omega_{k,\rm fid} = 1 - \Omega_{m,\rm fid} - \Omega_{\Lambda,\rm fid}$ curvature, and H_0 the present-day Hubble parameter. We have

$$\Omega_{m,\rm fid}(z) = \frac{\Omega_{m,0,\rm fid}(1+z)^3}{H^2_{\rm fid}(z)/H^2_{0,\rm fid}}, \tag{9}$$

where $\Omega_{m,0}$ refers to energy density evaluated at $z = 0$. In a Friedmann–Robertson–Walker universe the solution for the linear growth factor $D_{\rm fid}(z)$ and the dimensionless linear growth rate f are given by

$$g_{\rm fid}(\Omega_{m,\rm fid}(z)) \equiv \frac{D_{\rm fid}(z)}{a} = \frac{5\Omega_{m,\rm fid}(z)H^3_{\rm fid}(z)}{2(1+z)^2}\int_z^\infty {\rm d}z' \frac{(1+z')}{H^3_{\rm fid}(z')} \tag{10}$$

with scalefactor a;

$$f_{\rm fid}(\Omega_{m,\rm fid}(z)) = -1 - \frac{\Omega_{m,\rm fid}(z)}{2} + \Omega_{\Lambda,\rm fid}(z) + \frac{5\Omega_{m,\rm fid}(z)}{2g_{\rm fid}(z)}. \tag{11}$$

Under the assumption of a flat universe i.e. $\Omega_{k,\rm fid} = 0$, we have $\Omega_{\Lambda,\rm fid}(z) = 1 - \Omega_{m,\rm fid}(z)$.

For the fiducial galaxy bias model we choose a simple ad hoc functional form as used in Rassat et al. (2008), which is approximately correct for the Hα galaxies to be observed by the Euclid survey,

$$b_{\rm fid} = \sqrt{1+z}. \tag{12}$$

3.2 Parametrizing deviations

The derivation presented in Section 2 required us to define the parameters that we wish to optimize measurement of. We wish to choose parameters that allow us to measure deviations from the ΛCDM model. In the absence of compelling alternative cosmological models, we choose parameters that define an expansion in redshift of the cosmological behaviour we wish to understand – in our case the structure growth rate and the expansion rate. Both of these can be modelled by deviations in $\Omega_m(z)$ away from the fiducial model, and we adopt this quantity as the redshift-evolving quantity that we wish to understand, rather than the distance–redshift relation considered by Zhu et al. (2015), which does not easily extend to structure growth differences. We expand $\Omega_m(z)$ around the fiducial model as,

$$\frac{\Omega_m(z)}{\Omega_{m,\rm fid}(z)} = q_0\left(1 + q_1 y(z) + \frac{1}{2}q_2 y(z)^2\right), \tag{13}$$

we fix a pivot redshift $z_{\rm p}$ within the survey redshift range and y is defined as $y(z) + 1 \equiv \frac{\Omega_{m,\rm fid}(z)}{\Omega_{m,\rm fid}(z_{\rm p})}$; the expansion parameters q_0, q_1 and q_2 are obtained from equation (13) and its first and second derivatives evaluated at $z_{\rm p}$;

$$q_0 = \frac{\Omega_m(z_{\rm p})}{\Omega_{m,\rm fid}(z_{\rm p})},$$

$$q_1 = \frac{\Omega_{m,\rm fid}(z_{\rm p})}{\Omega_m(z_{\rm p})}\frac{{\rm d}\Omega_m/{\rm d}z|_{z_{\rm p}}}{{\rm d}\Omega_{m,\rm fid}/{\rm d}z|_{z_{\rm p}}} - 1,$$

$$q_2 = \left[\frac{\Omega_{m,\rm fid}(z_{\rm p})}{\Omega_m(z_{\rm p})}\frac{{\rm d}^2\Omega_m}{{\rm d}z^2}\Big|_{z_{\rm p}} - \frac{{\rm d}^2\Omega_{m,\rm fid}}{{\rm d}z^2}\Big|_{z_{\rm p}} - \left(\frac{\Omega_{m,\rm fid}(z_{\rm p})}{\Omega_m(z_{\rm p})}\frac{{\rm d}\Omega_m/{\rm d}z|_{z_{\rm p}}}{{\rm d}\Omega_{m,\rm fid}/{\rm d}z|_{z_{\rm p}}} - 1\right)\left(\frac{2}{\Omega_{m,\rm fid}(z_{\rm p})} \times \left(\frac{{\rm d}\Omega_{m,\rm fid}}{{\rm d}z}\right)^2\Big|_{z_{\rm p}} + \frac{{\rm d}^2\Omega_{m,\rm fid}}{{\rm d}z^2}\Big|_{z_{\rm p}}\right)\right]\frac{\Omega_{m,\rm fid}(z_{\rm p})}{\left({\rm d}\Omega_{m,\rm fid}/{\rm d}z|_{z_{\rm p}}\right)^2}. \tag{14}$$

The Hubble parameter with respect to $\Omega_m(z)$ is

$$\frac{H^2(z)}{H_0^2} = \frac{\Omega_{m,0}(1+z)^3}{\Omega_m(z)}, \tag{15}$$

where we have assumed that the dark matter equation of state is fixed,

$$\mathcal{P} = w\rho; \qquad w = 0 \tag{16}$$

with pressure $\mathcal{P}$ and matter density ρ.

A broader range of models could be derived by perturbing the homogeneous solution of the Einstein equations, but in this work we restrict ourselves to deviations close to ΛCDM in the dark energy and curvature components. The Ω_m parametrization allows for many deviations from ΛCDM: all the standard cosmological parameters can be written in terms of the q_i parameters e.g. if we want to allow for modified gravity models we can parametrize the growth factor as a function of $\Omega_m(z)$. Alternatively, if we are studying the deviations from a fiducial geometry we can parametrize the AP parameters. We assume that equations (10) and (11) hold for the perturbed $\Omega_m(z)$, which fix how the parameters q_i lead to deviations in the growth rate away from the fiducial model.

4 REDSHIFT WEIGHTING ASSUMING KNOWN DISTANCE–REDSHIFT RELATION

In this section, we derive a set of optimal weights to measure $\Omega_m(z)$ and the bias when the distance–redshift relation is assumed known, i.e. we derive the weights for an observed power spectrum that contains only the distortion due to RSD and not due to the AP effect.

We will discuss three different cases with different assumptions about parameters assumed known: the first two aim to estimate $\Omega_m(z)$ and the third the bias, parametrized by $b\sigma_8(z)$. In Section 4.2, we consider the case in which the bias is known and fixed to

a fiducial model; in this case we are considering that the information about Ω_m is coming from all the terms of the power-spectrum multipoles. We discuss this set of weight with respect to different fiducial models for the bias in order to test how knowing the bias would affect the results. However, this first set of weights does not match the actual RSD measurements condition in which the bias is unknown. We then consider in Section 4.3 a case for RSD measurements where we assume the growth information is not coming from tangential power and the only information to be considered comes from $f\sigma_8$. Bias evolution plays an important role for clustering measurements even if, in the redshift range of interest for future and current surveys, Ω_m is significantly more sensitive to redshift than bias, (see Section 3). As our last case, in Section 4.4, we consider for completeness a set of weight to measure the bias relation as a function of redshift.

4.1 Modelling the observed power spectrum

For simplicity we adopt a linear model for the RSDs, assume that we are working in the plane parallel approximation, and assume a linear deterministic bias model so that the power spectrum in redshift space, P^s is related to the real power spectrum P by

$$P^s(\boldsymbol{k}) = (b + f\mu_{\mathbf{k}}^2)^2 P(k) \tag{17}$$

where $P(k)$ is the linear real space power spectrum and where $\mu_{\mathbf{k}} \equiv \hat{\boldsymbol{z}} \cdot \hat{\boldsymbol{k}}$ is the cosine of the angle between the wavevector $\boldsymbol{k}$ and the line of sight $\hat{\boldsymbol{z}}$, (Kaiser 1987).

It is common to decompose P^s into an orthonormal basis of Legendre polynomials such that, in a linear regime, the redshift power spectrum is well described by its first three non-null moments: monopole P_0, quadrupole P_2 and hexadecapole P_4.

$$P^s(\boldsymbol{k}) = \mathcal{P}_0(\mu_{\mathbf{k}})P_0(k) + \mathcal{P}_2(\mu_{\mathbf{k}})P_2(k) + \mathcal{P}_4(\mu_{\mathbf{k}})P_4(k), \tag{18}$$

related with $P(k)$ through,

$$P_0(k) = \left(b^2 + \frac{2}{3}bf + \frac{1}{5}f^2\right) P(k), \tag{19}$$

$$P_2(k) = \left(\frac{4}{3}bf + \frac{4}{7}f^2\right) P(k) \quad \text{and} \tag{20}$$

$$P_4(k) = \left(\frac{8}{35}f^2\right) P(k). \tag{21}$$

We normalize the power spectrum using the standard variance of the galaxy distribution smoothed on scale $R = 8\,h^{-1}$Mpc, $\sigma_8(z)$, where

$$\sigma_8(z) = \sigma_{8,0} D(z) = \sigma_{8,0} \frac{g(z)}{1+z}. \tag{22}$$

This normalization enters into equation (17) in a way that is perfectly degenerate with b and f, which could be replaced by new parameters $(b\sigma_8)$ and $(f\sigma_8)$.

4.2 Optimal weights to measure $\Omega_m(z)$ assuming known bias

We build optimal weights by taking the derivative of the power-spectrum model with respect to the parameters q_i, As discussed in Section 2, hereafter we only consider the component of these weights that varies with $P_{,i}$, which we denote for the monopole, quadrupole and hexadecapole, respectively, $\boldsymbol{w}_0$, $\boldsymbol{w}_2$, and $\boldsymbol{w}_4$. For simplicity we refer to these as the 'weights', but it is worth remembering that there is a missing inverse variance component.

$$w_{\ell,q_i} = \frac{\partial P_\ell}{\partial q_i}. \tag{23}$$

We explicitly write the redshift dependence of P on the q_i parameters, so that the right-hand side of equation (23) becomes

$$\frac{\partial P_\ell}{\partial q_i} = \frac{\partial P_\ell}{\partial f}\frac{\partial f}{\partial q_i} + \frac{\partial P_\ell}{\partial \sigma_8}\frac{\partial \sigma_8}{\partial q_i}. \tag{24}$$

This second term assumes that we are recovering information from both radial and transverse modes. This is true for the transverse component if the bias is known perfectly. We build our set of weights as a function of redshift, for the monopole we have

$$w_{0,i} = \left(\frac{2}{3}b + \frac{2}{5}f\right)\sigma_8^2\frac{\partial f}{\partial q_i} + \left(b^2 + \frac{2}{3}bf + \frac{1}{5}f^2\right)2\sigma_8\frac{\partial \sigma_8}{\partial q_i} \tag{25}$$

with

$$\frac{\partial f(z)}{q_i} = \frac{\partial \Omega_m(z)}{\partial q_i}\left(\frac{5}{2g(z)} - \frac{1}{2}\right) - \frac{\partial \Omega_m(z)}{\partial q_i} - \frac{5}{2}\frac{\Omega_m(z)}{g^2(z)}\frac{\partial g(z)}{\partial q_i}, \tag{26}$$

$$\frac{\partial \sigma_8(z)}{\partial q_i} = \frac{\sigma_{8,0}}{1+z}\frac{\partial g(z)}{\partial q_i}; \tag{27}$$

where

$$\begin{aligned}\frac{\partial g(z)}{\partial q_i} = {} & \frac{5}{2(1+z)^2}\left(\frac{\partial \Omega_m(z)}{\partial q_i}H^3(z) + 3H^2(z)\frac{\partial H(z)}{\partial q_i}\Omega_m(z)\right)\cdot \\ & \times \int_z^\infty \mathrm{d}z' \frac{(1+z')}{H^3(z')} - \frac{15\Omega_m(z)H^3(z)}{2(1+z)^2} \\ & \times \int_z^\infty \mathrm{d}z' \frac{(1+z')}{H^4(z')}\frac{\partial H(z')}{\partial q_i}\end{aligned} \tag{28}$$

$$\begin{aligned}\frac{\partial H(z)}{\partial q_i} = {} & H_0\frac{1}{2}\left(\frac{\Omega_{m,0}(1+z)^3}{\Omega_m(z)}\right)^{-1/2}\frac{(1+z)^3}{\Omega_m(z)} \\ & \cdot\left(\frac{\partial \Omega_{m,0}}{\partial q_i} - \frac{\Omega_{m,0}}{\Omega_m}\frac{\partial \Omega_m(z)}{\partial q_i}\right),\end{aligned} \tag{29}$$

with

$$\begin{aligned}\frac{\partial \Omega_m}{\partial q_0} &= \Omega_{m,\mathrm{fid}}(z), \\ \frac{\partial \Omega_m}{\partial q_1} &= \Omega_{m,\mathrm{fid}}(z)y(z), \\ \frac{\partial \Omega_m}{\partial q_2} &= \Omega_{m,\mathrm{fid}}(z)\frac{y^2(z)}{2}.\end{aligned} \tag{30}$$

Note that in the equations above the $P(k)$ term has been factored out; all the terms are evaluated at $q_0 = 1$ since we are ignoring the weights dependence on cosmology.

Similarly for the quadrupole and for the hexadecapole

$$\begin{aligned}w_{2,q_i} &= \left(\frac{4}{3}b + \frac{8}{7}f\right)\sigma_8^2\frac{\partial f}{\partial q_i} + \left(\frac{4}{3}bf + \frac{4}{7}f^2\right)2\sigma_8\frac{\partial \sigma_8}{\partial q_i}, \\ w_{4,i} &= \frac{16}{35}f\sigma_8^2\frac{\partial f}{\partial q_i} + \frac{8}{35}f^2 2\sigma_8\frac{\partial \sigma_8}{\partial q_i}.\end{aligned} \tag{31}$$

Fig. 1 shows the set of weights for the monopole, quadrupole and hexadecapole, with a convenient normalization. All the plots

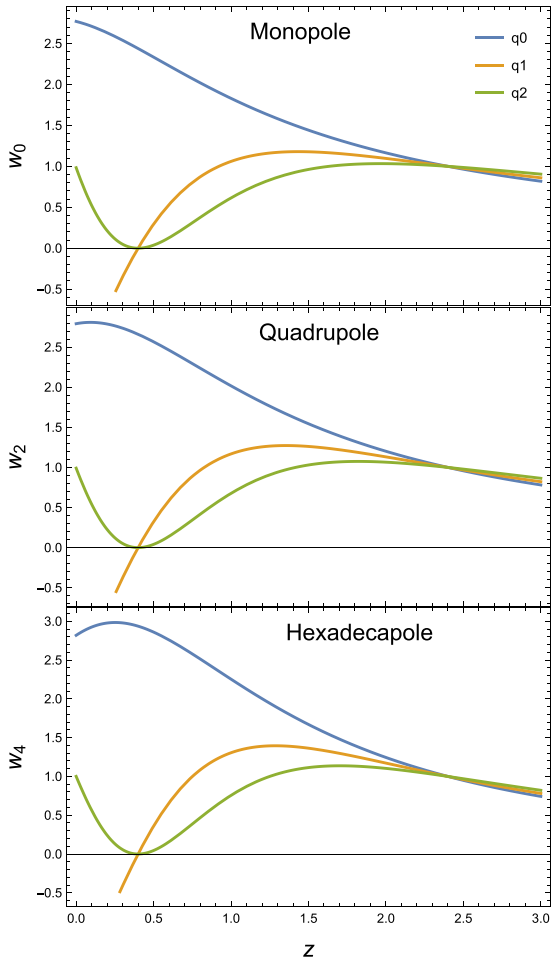

Figure 1. The weights for the monopole ($\boldsymbol{w}_0$), quadrupole ($\boldsymbol{w}_2$) and hexadecapole ($\boldsymbol{w}_4$) with respect to the q_i parameters: blue lines indicate the weight with respect to q_0, orange lines indicate the weight with respect to q_1 and the green lines indicate the weight with respect to q_2. These weights assume a fiducial bias evolving as $b = \sqrt{1+z}$ and were calculated for RSD measurements assuming that the bias is known, as described in Section 4.2.

are generated considering a ΛCDM model with $\Omega_{m,0} = 0.31$ as the fiducial cosmology. We explore a wide redshift range to see general trends, as if we are analysing data from a range of surveys. We fix a pivot redshift in $z_p = 0.4$. All three weights with respect to parameters q_0 (blue lines) show a peak at redshift $z \sim 0.1-0.2$; this is due to $\partial\Omega_m/\partial q_i$ term that rapidly grows until about $z \sim 2$ and then tends to a constant. The peak corresponds to the $\Omega_m \sim \Omega_\Lambda$ epoch: the weights aim to highlight the deviations from the fiducial cosmology ΛCDM, and therefore peak approximately in the range of the equivalence between matter and Λ. At higher redshifts the weights decrease due to the decreasing dependence of $\Omega_m(z)$ on f and σ_8.

The weights about the *slope parameters*, q_1 (orange line), rapidly grow at low redshift driven by $\partial\Omega_m/\partial q_1$ and $\partial P_\ell/\partial\sigma_8$, and then start decreasing as $\partial f/\partial\Omega_m$ and $\partial P_\ell/\Omega_m$ dominate. We see that they pickup small differences about the peak due to the different dependences on P_ℓ.

The green lines displays the weights with respect to the second-order parameter q_2: they are similar, with a minimum about $z \sim 0.5$: this difference with respect to q_0 and q_1 is due to the $\partial\Omega_m/\partial q_2$ term that starts decreasing with z until about $z \sim 0.4$ and then slowly increases. Comparing the monopole, quadrupole and hexadecapole weights we see that the weights behave in a similar way for all three statistics; the hexadecapole weights show a faster decrease for all three parameters, due to the absence of the bias dependence. However the differences with monopole and quadrupole are small, confirming our assumption that the bias choice does not drastically change the weights in the region of interest.

4.2.1 Application of the method

We have derived a set of weights that compress the information available in the power spectrum across a range of redshifts. In practice, to apply the method, we weight galaxies, assuming $\boldsymbol{w}_{\rm gal} = \sqrt{\boldsymbol{w}_{\delta^2}}$, to obtain a set of monopole, quadrupole and hexadecapole for each set of weights.

If we were only interested in a single parameter, (e.g. q_0) and we thought all the information came from the monopole, we would measure the weighted $P_{\boldsymbol{w},0}$ by applying the w_{0,q_0} to each galaxy; we would then fit q_0 by comparing the data with the theoretical prediction for the monopole, weighted at different redshifts as

$$P_{0,w_{0,q_0}\rm model}(k) = \int {\rm d}z\ P_0(k,z)\cdot w_{0,q_0}(z). \quad (32)$$

Where the $P_0(k, z, q_0)$ corresponds to the monopole prediction, e.g. equation (19) and we have ignored the window effects. If we further assume the simple linear model for RSD, (Kaiser 1987),

$$P_0(k,z) = \left(b^2 + \frac{2}{3}bf(\Omega_m(q_0,z)) + \frac{1}{5}f(\Omega_m(q_0,z))^2\right)P(k); \quad (33)$$

we can express f in terms of $\Omega_m(q_0, z)$ according to equation (11).

In order to simultaneously measure all three q_i parameters, we measure each multipole weighted to be optimal for each q_i parameters, i.e. we weight galaxies with the different w_{i,q_j} functions and we build a data vector Π as,

$$\Pi^{\rm T} = (P_{0,w_{0,q_0}}, P_{0,w_{0,q_1}}, P_{0,w_{0,q_2}}\ \ldots\ P_{4,w_{4,q_2}})^{\rm T}. \quad (34)$$

Note that each weighted multipole $P_{i,w_{i,q_j}}$ provides a particular piece of information about $\Omega_m(z)$ that optimizes the measurement of each q_i. We constrain the three q_i by jointly fitting from the data-vector Π compared with a $\Pi_{\rm model}$. In practice we assume a Gaussian likelihood and minimize

$$\chi^2 \propto (\Pi - \Pi_{\rm model})^{\rm T} C^{-1} (\Pi - \Pi_{\rm model}); \quad (35)$$

where each $P_{i,w_{i,q_j}}$ inside $\Pi_{\rm model}$ is modelled as in equation (32). The $\mathbf{C}^{-1}$ term corresponds to the joint covariance matrix.

4.2.2 The dependence on the fiducial bias model

We now test the robustness of the set of weights for Ω_m, presented in Section 4.2, with respect to the bias model. To do this, we compute sets of weights from different choices of $b(z)$. We first derive the set of weights presented in Section 4, parametrized with respect to Ω_m, fixing a constant bias, $b = 1.024$, which is our fiducial value at $z = 0.45$, then we repeat for $b = 1/D_{\rm fid}(z)$.

Figs 2 and 3 show that the behaviour of the weights with redshift is similar to previous results and there are no significant differences in the shapes. As expected the differences are more visible in the monopole (top panel) than in the quadrupole (bottom panel) since the former is more sensitive to galaxy bias. We exclude the weights for the hexadecapole since it does not depend on galaxy bias.

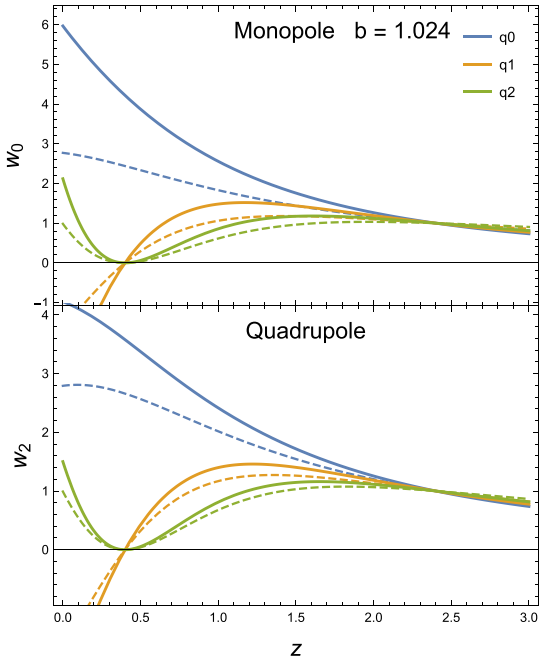

Figure 2. Solid lines as Fig. 1, but assuming a constant bias $b = 1.024$. We compare this set of weights with the results presented in Fig 1, (dashed lines), obtained assuming a bias evolving as $b = \sqrt{1+z}$.

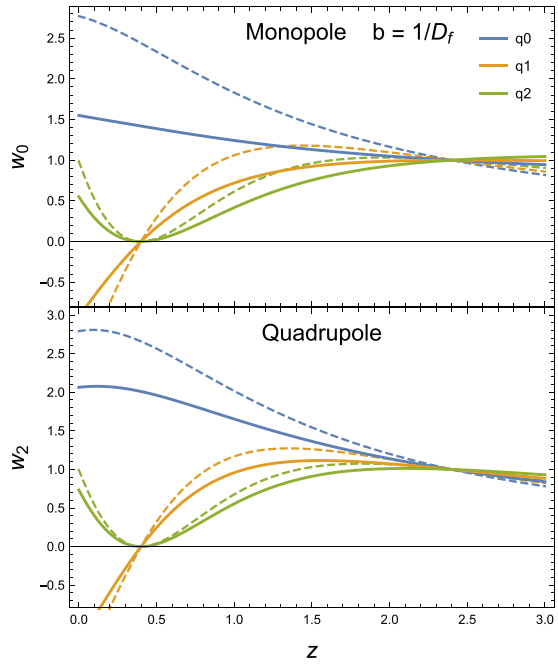

Figure 3. Solid lines as Fig. 1, but assuming a fiducial bias evolving with redshift as $b = 1/D_{\rm f}(z)$. We compare this set of weights with the results presented in Fig 1, (dashed lines), obtained assuming a bias evolving as $b = \sqrt{1+z}$.

4.3 Optimal weights to measure $\Omega_m(z)$ with unknown bias

RSD measurements constrain the product of the two key parameters f and σ_8 and it is common to consider a single measurement of $[f\sigma_8]$, marginalizing over an unknown bias. Therefore we present a set of weights that matches the philosophy of current RSD measurements:

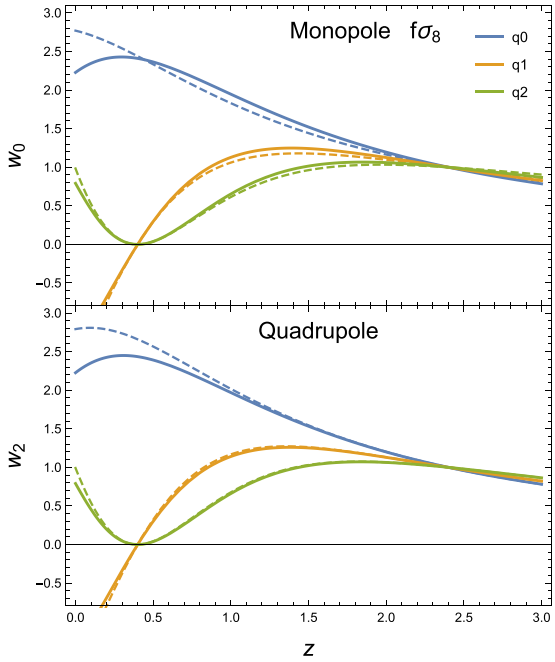

Figure 4. Solid lines show weights for the monopole (w_0) quadrupole (w_2) and hexadecapole (w_4), with respect to the q_i parameters ignoring the information in $b\sigma_8$ term, as described in Section 4.3. These are compared with the weights presented in Fig. 1 (dashed lines), which assume that the bias is known.

we consider the term $[b\sigma_8]$ to be *independent* from $[f\sigma_8]$ since we marginalize over the bias.

Considering e.g. the monopole

$$P_0 = \left([b\sigma_8]^2 + \frac{2}{3}[b\sigma_8][f\sigma_8](z) + \frac{1}{5}[f\sigma_8]^2(z)\right)P(k)\Big/\left(\sigma_8^2\right) \quad (36)$$

for unknown bias the dependence on the q_i parameters is only through $[f\sigma_8]$. We derive the set of weight by taking the derivative of P_0, P_2, P_4 with respect to q_1, q_2, q_3,

$$w_{0,q_i} \equiv \left(\frac{2}{3}[b\sigma_8] + \frac{2}{5}[f\sigma_8](z)\right)\frac{\partial[f\sigma_8]}{\partial q_i}(z), \quad (37)$$

$$w_{2,q_i} \equiv \left(\frac{4}{3}[b\sigma_8] + \frac{8}{7}[f\sigma_8](z)\right)\frac{\partial[f\sigma_8]}{\partial q_i}(z), \quad (38)$$

$$w_{4,q_i} \equiv \left(\frac{16}{35}[f\sigma_8](z)\right)\frac{\partial[f\sigma_8]}{\partial q_i}(z), \quad (39)$$

where the derivatives $\partial[f\sigma_8]/\partial q_i(z)$ are obtained using equations (26) and (27).

Fig. 4 shows the set of weights for the monopole, quadrupole and hexadecapole parametrized with respect to q_0, q_1, and q_2, when ignoring the information contained in $[b\sigma_8]$, conveniently normalized. We compare them with the weights derived in Section 4.2, presented in Fig. 1, (dashed lines). The main difference between the two set of weights lies on the assumptions we make for galaxy bias: if we are setting it as completely unknown, considering only the information contained in $[f\sigma_8]$ or if we are including $[b\sigma_8]$ term, constraining $b(z)$ to a fiducial model; however the plots show a very similar behaviour between the two cases, it is clear then that the tangential modes do not play a large role in determining optimal weights.

4.4 Optimal weights to measure bias

For completeness we will show how to derive weights that optimally measure the evolution of the bias parameter around the fiducial model.

In an analogous manner to equation (13) we model $[b\sigma_8](z)$ as an expansion about a fiducial model $[b\sigma_8]_{\rm fid}$:

$$\frac{[b\sigma_8](z)}{[b\sigma_8]_{\rm fid}(z)} = \eta_0 \left(1 + \eta_1 x + \frac{1}{2}\eta_2 x^2\right) \tag{40}$$

about a pivot redshift $z_{\rm p}$, where $1 + x \equiv \frac{[b\sigma_8]_{\rm fid}(z)}{[b\sigma_8]_{\rm fid}(z_p)}$.

The η parameters correspond to the derivative 0, 1, 2 of $[b\sigma_8](z)$ relation evaluated at $z_{\rm p}$.

In analogy with measuring q_i, we can derive a set of weights that optimally estimate the bias-redshift through the η_j parameters,

$$w_{\ell,\eta_j} = \frac{\partial P_\ell}{\partial [b\sigma_8]} \frac{\partial [b\sigma_8]}{\eta_j}. \tag{41}$$

This set of weights can be applied instead of the set of weights with respect to Ω_m in case we want to measure deviations from the fiducial model chosen for the bias. We do not plot these weights for simplicity but include the derivation to show how they could be calculated.

5 REDSHIFT WEIGHTING ASSUMING UNKNOWN DISTANCE–REDSHIFT RELATION

Our previous results provide an optimal scheme specific for RSD measurements; as pointed out in the introduction it would be very useful to optimize at the same time geometric measurements and thus enable measurements that include all the parameters both for computational costs and accuracy of the results. An optimal weighted scheme for BAO measurements has been recently presented in Zhu et al. (2015) where the authors describe a weighting scheme parametrized with respect to the distance–redshift relation, including the AP effect modelled as

$$\begin{aligned} k_\perp &\rightarrow \alpha^{-1}(1+\epsilon)k_\perp, \\ k_\parallel &\rightarrow \alpha^{-1}(1+\epsilon)^{-2}k_\parallel, \end{aligned} \tag{42}$$

with parameters, α, for isotropic deformation and, ϵ, for anisotropic. The method optimizes only BAO measurements, constraining the covariance matrix at BAO scales and ignoring the growth parameters.

In this section, we will account for both distortions due to peculiar velocities and distortions due to incorrect choice of geometry described by the AP effect. We still use a parametrization of $\Omega_m(z)$ to define deviations from our fiducial model as described in equation (13).

5.1 Modelling AP and RSD in the observed $P(k)$

We denote k^t and k the true and observed coordinates, respectively, then assuming that an incorrect geometry transforms the coordinates

$$\begin{aligned} k^t &= \frac{k}{\alpha_\perp}\left[1 + \mu^2\left(\frac{\alpha_\perp^2}{\alpha_\parallel^2} - 1\right)\right]^{1/2}, \\ \mu^t &= \mu\frac{\alpha_\perp}{\alpha_\parallel}\left[1 + \mu^2\left(\frac{\alpha_\perp^2}{\alpha_\parallel^2} - 1\right)\right]^{-1/2}, \end{aligned} \tag{43}$$

with $\alpha_\parallel$ defined as the ratio between the observed and the true Hubble parameter, $H(z)/H_t(z)$ and $\alpha_\perp$ defined as the ratio between the true and the observed angular diameter distance $D_{A,t}(z)\,/\,D_A(z)$, e.g. (Ballinger, Peacock & Heavens 1996); the multipoles at the observed k are related to the power spectrum at k^t, through

$$P_\ell(k) = \frac{2\ell+1}{2}\int_{-1}^{1} {\rm d}\mu\, P(k^t, \mu^t)\mathcal{L}_\ell(\mu). \tag{44}$$

For linear RSD, Kaiser (1987), inserting the transformation of the coordinates given by equation (43), the galaxy power spectrum at the true wavenumber is

$$\begin{aligned} P^s(k^t, \mu^t) = {} & \frac{1}{\alpha_\perp^2\alpha_\parallel} P\left[\frac{k}{\alpha_\perp}\left[1 + \mu^2\left(\frac{\alpha_\perp^2}{\alpha_\parallel^2} - 1\right)\right]^{1/2}\right] \\ & \times \left[1 + \mu^2\left(\frac{\alpha_\perp^2}{\alpha_\parallel^2} - 1\right)\right]^{-2}\left\{1 + \mu^2\left[(\beta+1)\frac{\alpha_\perp^2}{\alpha_\parallel^2} - 1\right]\right\}^2. \end{aligned} \tag{45}$$

We use the notation $\beta \equiv f/b$ for simplicity with equations.

We expand first order P in the right-hand side of equation (45), in order to get analytical derivatives with respect to the expansion parameters. We have tested numerically that this approximation does not influence our conclusions.

Introducing $\varphi \equiv \frac{\alpha_\perp^2}{\alpha_\parallel^2} - 1$, we can expand the right-hand side of equation (45) to first order about $(\alpha_\perp, \varphi) = (1, 0)$, using

$$\begin{aligned} P\left[\frac{k}{\alpha_\perp}\left(1 + \mu^2\varphi\right)^{1/2}\right] \approx {} & P(k) \\ & + (\alpha_\perp - 1)\left.\frac{\partial P}{\partial k}\frac{\partial k}{\partial k^t}\frac{\partial k^t}{\partial \alpha_\perp}\right|_{\substack{\alpha_\perp=1\\ \varphi=0}} + \varphi\left.\frac{\partial P}{\partial k}\frac{\partial k}{\partial k^t}\frac{\partial k^t}{\partial \varphi}\right|_{\substack{\alpha_\perp=1\\ \varphi=0}}. \end{aligned} \tag{46}$$

Substituting in equation (45) and then in equation (44), we obtain models of the multipoles accounting for both RSD and AP effects to be

$$\begin{aligned} P_\ell(k) = {} & \frac{2\ell+1}{2}\int_{-1}^{1} {\rm d}\mu\,\mathcal{L}_\ell(\mu)\Big\{P(k)\left(1 + \mu^2\beta\right)^2 \\ & + \varphi\left[\frac{1}{2}\frac{\partial P}{\partial \ln k}\mu^2\left(1 + \mu^2\beta\right)^2 + P(k)(-2\mu^2)(1 + \beta\mu^2)^2\right. \\ & \left. + 2\mu^2(1 + \beta\mu^2)(1 + \beta)P(k) - \frac{1}{2}P(k)(1 + \mu^2\beta)^2\right] \\ & + (1 - \alpha_\perp)(1 + \mu^2\beta)^2\left(\frac{\partial P}{\partial \ln k} + 3P(k)\right)\Big\}. \end{aligned} \tag{47}$$

In particular it holds that $P^s(k)$ at a linear order is described by the first three multipoles (Ross et al. 2015). The monopole, quadrupole and hexadecapole are

$$\begin{aligned} P_0(k) = {} & \frac{1}{2}\sigma_8^2\Big\{\left(2 + \frac{4}{3}\beta + \frac{2}{5}\beta^2\right)P(k) + \varphi\Big[\left(\frac{1}{3} + \frac{2}{5}\beta + \frac{1}{7}\beta^2\right) \\ & \times \frac{\partial P}{\partial \ln k} - \left(1 + \frac{2}{15}\beta - \frac{1}{35}\beta^2\right)P(k)\Big] \\ & + (1 - \alpha_\perp)\left(2 + \frac{4}{3}\beta + \frac{2}{5}\beta^2\right)\left(\frac{\partial P}{\partial \ln k} + 3P(k)\right)\Big\}, \\ P_2(k) = {} & \frac{5}{2}\sigma_8^2\Big\{\left(\frac{8}{15}\beta + \frac{8}{35}\beta^2\right)P(k) + \varphi\Big[\left(\frac{2}{15} + \frac{8}{35}\beta\right. \end{aligned}$$

$$+\frac{2}{21}\beta^2\Big)\frac{\partial P}{\partial \ln k}-\left(\frac{4}{21}\beta+\frac{4}{105}\beta^2\right)P(k)\Big]$$
$$+(1-\alpha_\perp)\left(\frac{8}{15}\beta+\frac{8}{35}\beta^2\right)\left(\frac{\partial P}{\partial \ln k}+3P(k)\right)\Big\},$$
$$P_4(k)=\frac{9}{2}\sigma_8^2\Big\{\frac{16}{315}\beta^2P(k)+\varphi\left[\left(\frac{16}{315}\beta+\frac{8}{231}\beta^2\right)\frac{\partial P}{\partial \ln k}$$
$$-\left(\frac{32}{315}\beta+\frac{24}{385}\beta^2\right)P(k)\right]$$
$$+(1-\alpha_\perp)\frac{16}{315}\beta^2\left(\frac{\partial P}{\partial \ln k}+3P(k)\right)\Big\}. \quad (48)$$

5.2 AP and RSD weights derivation, assuming known bias

As before, the weights for the power-spectrum multipoles, assuming information from both RSD and AP effects, are obtained by taking the derivative of the P_i with respect to the q_i parameters defined in Section 3.2,

$$w_{\ell,q_i}=\frac{\partial P_\ell}{\partial q_i}=\frac{\partial P_\ell}{\partial\varphi}\frac{\partial\varphi}{\partial q_i}+\frac{\partial P_\ell}{\partial\alpha_\perp}\frac{\partial\alpha_\perp}{\partial q_i}+\frac{\partial P_\ell}{\partial\beta}\frac{\partial\beta}{\partial f}\frac{\partial f}{\partial q_i}+\frac{\partial P_\ell}{\partial\sigma_8}\frac{\partial\sigma_8}{\partial q_i}. \quad (49)$$

all the derivatives are evaluated at the fiducial model. In case of flat universe we have

$$\alpha_\perp(z)=\frac{\int_0^z \mathrm{d}z' 1/H(q_i,z')}{\int_0^z \mathrm{d}z'' 1/H_{\rm fid}(z'')}. \quad (50)$$

Inserting the definition of β and φ,

$$\frac{\partial\beta}{\partial f}=\frac{1}{b},$$
$$\frac{\partial\varphi}{\partial q_i}=-\frac{2\alpha_\perp^3}{\alpha_\parallel^3}\left(\frac{1}{\alpha_\perp}\frac{\partial\alpha_\parallel}{\partial q_i}+\frac{-\alpha_\parallel}{\alpha_\perp^2}\frac{\partial\alpha_\perp}{\partial q_i}\right), \quad (51)$$

where

$$\frac{\partial\alpha_\parallel}{\partial q_i}=-\frac{1}{H_{\rm fid}(z)}\frac{\partial H}{\partial q_i},$$
$$\frac{\partial\alpha_\perp}{\partial q_i}=\frac{\int_0^z \mathrm{d}z'-\frac{1}{H_{\rm fid}^2(z')}\frac{\partial H}{\partial q_i}}{\int_0^z \mathrm{d}z''1/H_{\rm fid}(z'')}. \quad (52)$$

In Appendix A, we present the derivatives of the multipoles P_i with respect to φ, $\alpha_\perp$, f and σ_8.

The weights have arbitrary normalization but we cannot factor out the scale dependence as we did for the RSD weights since we now have two different k-dependent terms P and $\mathrm{d}P/\mathrm{d}\ln k$. However, Zhao et al. (in preparation) show that this dependence is very weak.

Fig. 5 shows the weights optimal for RSD and AP measurements evaluated at $k=0.1\ h\ \mathrm{MPc}^{-1}$, for the monopole, quadrupole and hexadecapole, respectively. Blue lines indicate the weights with respect to q_0, orange lines with respect to q_1 and green lines with respect to q_2. Comparing with the previous result that assumed a known distance–redshift relation (dashed lines), it is possible to see that the behaviour of the three weights does not change drastically. In general, the redshift dependence is stronger including also the AP effect and the new weights show a more enhanced maximum. Since the contribution from φ and $\alpha_\perp$ vanishes for q_0, the weights w_{i,q_0} are equivalent to the previous weights without the AP effect. (Fig 1).

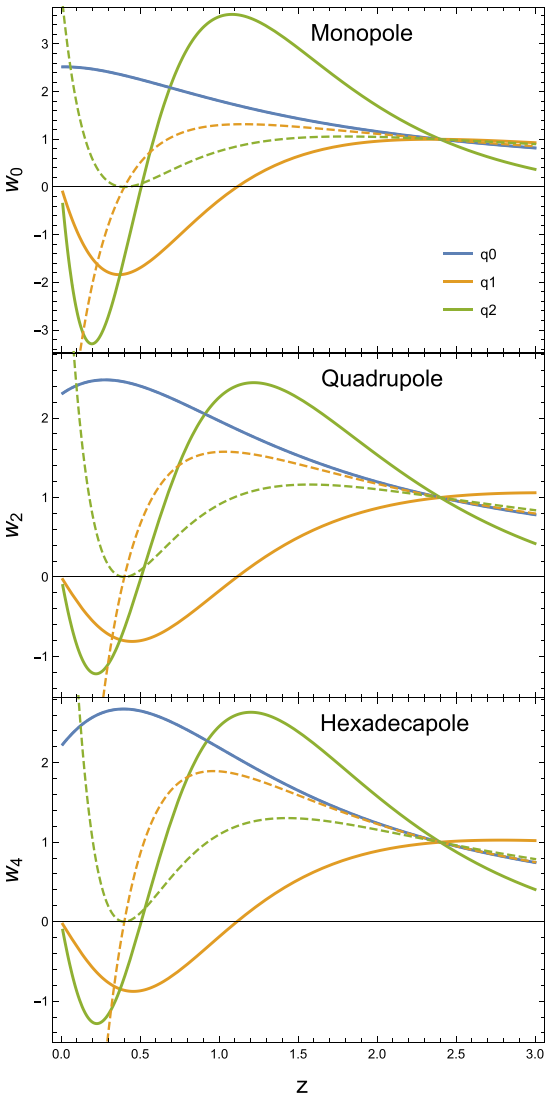

Figure 5. The RSD + AP optimal weights for the monopole $\boldsymbol{w}_0$, quadrupole $\boldsymbol{w}_2$ and hexadecapole $\boldsymbol{w}_4$. Blue lines indicate the weights with respect to the q_0 parameter. Orange lines indicate the weights with respect to the q_1 parameter and green lines indicates the weights with respect to the q_2 parameter. We compare them with previous results, where the distance–redshift relation was fixed (dashed lines); the weights w_{ℓ,q_0} (blue lines) are equivalent to the previous weights without the AP effect since the contribute from φ and $\alpha_\perp$ vanish because of $\partial H(q_i)/\partial q_0=0$. The RSD+AP weights show enhanced features due to the AP parameters, whose importance increases with redshift.

5.3 AP–RSD weights assuming unknown bias

If we now neglect the information given by $[b\sigma_8]$, as we did for one set of RSD weights, we substitute $\beta=f/b$, then we change the equation (52) to

$$w_{\ell,q_i}=\frac{\partial P_\ell}{\partial q_i}=\frac{\partial P_\ell}{\partial\varphi}\frac{\partial\varphi}{\partial_i}+\frac{\partial P_\ell}{\partial\alpha_\perp}\frac{\partial\alpha_\perp}{\partial q_i}+\frac{\partial P_\ell}{\partial f\sigma_8}\frac{\partial f\sigma_8}{\partial q_i}, \quad (53)$$

where we have assumed that $\partial[b\sigma_8]/\partial q_i=0$.

In Section 4, we showed that there are no significant differences between the cases in which $b\sigma_8$ is known and unknown, however, for the reasons discussed in Section 4, they are more consistent with

the RSD measurements. We do not plot any new results since the differences are very small.

6 DISCUSSION

In the first part of the paper, we presented a set of optimal redshift-dependent weights for RSD measurements. These functions allow us to optimally compress the original data set while minimizing the error a priori provided by the Fisher matrix, on the parameters we want to measure. In contrast to the current RSD measurements, which compare the data with the model at a single effective redshift, the weights presented account for the redshift evolution of the cosmological effects, since the measurements are now compared with a weighted model covering a range of redshifts. The method is based on a particular choice of a relation in redshift we want to measure/investigate, e.g. modelled as an expansion about a fiducial model. We derived the set of weights that optimally estimates deviations from a ΛCDM background, modelled using variations of $\Omega_m(z)$; we modelled $\Omega_m(z)$ as a polynomial expansion in terms of parameters q_i about a fixed fiducial models $\Omega_{m,\mathrm{fid}}$, then we applied the compression method as described in Tegmark et al. (1997) and derived the set of weights that optimally estimates the expansion parameters. As explained in Section 2, our weights generalize the FKP weights: they take in account of the galaxy density distribution through the covariance matrix and allow sensitivity to the redshift dependence of the statistics we are measuring.

We started assuming a known distance–redshift relation and considering two different cases: one in which the bias is known and constrained to a fiducial model and one in which the bias is unknown and we marginalize over it. We compared them and we showed the consistency between the two schemes: this means that the bias does not play a large role in determining the weights. We also tested our assumptions on the fiducial bias model by deriving the previous results for two different bias models. We also confirmed in this case that the weights are not significantly sensitive to $b(z)$. For completeness we presented a further set of weights that optimize the measurement of bias.

In order to improve future measurements we extended the previous weights to a more general case, when the distance–redshift relation is unknown: we modelled the observed power spectrum including the AP effect; we introduced two new distortion parameters φ and $\alpha_\perp$ in $P(k)$ describing the AP effect. The set of weights obtained for the RSD and AP measurements is scale dependent through the ratio of $P(k)$ and its logarithmic derivative. This is not a particular issue for future applications since this dependence is predicted to be very weak, moreover considering e.g. CAMB (Lewis & Bridle 2002) computing $P(k)$ model in real space or its derivative will not require high computational time, provided we apply these weights after calculating the power. Zhu et al. did not face this problem since they constrained every quantity on the BAO scale ($k \sim 0.1\,h\,\mathrm{Mpc}^{-1}$). We compared the new results with the weights accounting for RSD only at BAO scale showing that the redshift dependence is now increased by the inclusion of the AP parameters.

In order to correctly apply the weighting scheme we will need to understand how to combine with weights designed to correct for systematic density field distortions. The derivations presented made a number of assumptions (e.g. the fact that the power-spectrum shape is equal for each redshift slice and that P is Gaussian distributed). It would be interesting to see if the weights change when we relax these assumptions – we leave this for future work.

ACKNOWLEDGEMENTS

RR and WJP acknowledge support from the European Research Council through grant *Darksurvey*. WJP is also grateful for support from the UK Science & Technology Facilities Council through the consolidated grant ST/K0090X/1 and support from the UK Space Agency through grant ST/K00283X/1. HGM acknowledges the Agence Nationale de la Recherche, as part of the programme Investissements d'avenir under the reference ANR-11-IDEX-0004-02. GBZ and YW are supported by the Strategic Priority Research Program 'The Emergence of Cosmological Structures' of the Chinese Academy of Sciences Grant No. XDB09000000.

REFERENCES

Ballinger W. E., Peacock J. A., Heavens A. F., 1996, MNRAS, 282, 877
Bianchi D., Gil-Marín H., Ruggeri R., Percival W. J., 2015, MNRAS, 453, L11
Eisenstein D. J., Seo H.-J., White M., 2007, ApJ, 664, 660
Feldman H. A., Kaiser N., Peacock J. A., 1994, ApJ, 426, 23
Gil-Marín H. et al., 2016, MNRAS, 460, 4210
Hamilton A. J. S., 1998, in Hamilton D., ed., Astrophysics and Space Science Library, Vol. 231, The Evolving Universe. Springer-Verlag, Berlin, p. 185
Kaiser N., 1987, MNRAS, 227, 1
Kalus B., Percival W. J., Samushia L., 2016, MNRAS, 455, 2573
Laureijs R. et al., 2011, preprint (arXiv:1110.3193)
Levi M. et al., 2013, preprint (arXiv:1308.0847)
Lewis A., Bridle S., 2002, Phys. Rev. D, 66, 103511
Percival W. J., Verde L., Peacock J. A., 2004, MNRAS, 347, 645
Pope A., Szalay A., Matsubara T., Blanton M. R., Eisenstein D. J., Gray J., Jain B., 2004, in Allen R. E., Nanopoulos D. V., Pope C. N., eds, AIP Conf. Proc. Vol. 743, The New Cosmology: Conference on Strings and Cosmology. Am. Inst. Phys., New York, p. 120
Rassat A. et al., 2008, preprint (arXiv:0810.0003)
Ross A. J. et al., 2015, in American Astronomical Society Meeting Abstracts, Vol. 225, p. 125.02
Scoccimarro R., 2015, Phys. Rev. D, 92, 083532
Tegmark M., Taylor A. N., Heavens A. F., 1997, ApJ, 480, 22
Vogeley M. S., Szalay A. S., 1996, ApJ, 465, 34
Zhu F., Padmanabhan N., White M., 2015, MNRAS, 451, 236

APPENDIX A: DERIVATIVE OF THE MULTIPOLES WITH RESPECT TO φ, $\alpha_\perp$, β, σ_8

We here present the derivatives of the generalized multipoles computed in Section 5.1, with respect to the redshift-dependent parameters:

$$\frac{\partial P_0}{\partial \varphi} = \frac{1}{2}\sigma_8^2\left[\left(\frac{1}{3}+\frac{2}{5}\beta+\frac{1}{7}\beta^2\right)\frac{\partial P}{\partial \ln k} - \left(1+\frac{2}{15}\beta-\frac{1}{35}\beta^2\right)P(k)\right]$$

$$\frac{\partial P_0}{\partial \alpha_\perp} = -\frac{1}{2}\sigma_8^2\left(2+\frac{4}{3}\beta+\frac{2}{5}\beta^2\right)\left(\frac{\partial P}{\partial \ln k}+3P(k)\right)$$

$$\frac{\partial P_0}{\partial \beta} = \frac{1}{2}\sigma_8^2\left\{\left(\frac{4}{3}+\frac{4}{5}\beta\right)P(k)\right.$$

$$\frac{\partial P_0}{\partial \sigma_8} = \sigma_8\left(2+\frac{4}{3}\beta+\frac{2}{5}\beta^2\right)P(k) \qquad \text{(A1)}$$

$$\frac{\partial P_2}{\partial \varphi} = \frac{5}{2}\sigma_8^2\left[\left(\frac{2}{15}+\frac{8}{35}\beta+\frac{2}{21}\beta^2\right)\frac{\partial P}{\partial \ln k} - \left(\frac{4}{21}\beta+\frac{4}{105}\beta^2\right)P(k)\right]$$

$$\frac{\partial P_2}{\partial \alpha_\perp} = -\frac{5}{2}\sigma_8^2\left(\frac{8}{15}\beta+\frac{8}{35}\beta^2\right)\left(\frac{\partial P}{\partial \ln k}+3P(k)\right)$$

$$\frac{\partial P_2}{\partial \beta} = \frac{5}{2}\sigma_8^2\left(\frac{8}{15}+\frac{16}{35}\beta\right)P(k)$$

$$\frac{\partial P_2}{\partial \sigma_8} = 5\sigma_8\left(\frac{8}{15}\beta+\frac{8}{35}\beta^2\right)P(k) \tag{A2}$$

$$\frac{\partial P_4}{\partial \varphi} = \frac{9}{2}\sigma_8^2\left[\left(\frac{16}{315}\beta+\frac{8}{231}\beta^2\right)\frac{\partial P}{\partial \ln k} - \left(\frac{32}{315}\beta+\frac{24}{385}\beta^2\right)P(k)\right]$$

$$\frac{\partial P_4}{\partial \alpha_\perp} = -\frac{9}{2}\sigma_8^2\left\{\frac{16}{315}\beta^2\left(\frac{\partial P}{\partial \ln k}+3P(k)\right)\right\}$$

$$\frac{\partial P_4}{\partial \beta} = \frac{9}{2}\sigma_8^2\frac{32}{315}\beta P(k)$$

$$\frac{\partial P_4}{\partial \sigma_8} = 9\sigma_8\frac{16}{315}\beta^2 P(k). \tag{A3}$$

In case we wish to neglect the $[b\sigma_8]$ term, we need to substitute the derivatives with respect to β and σ_8, with the derivatives $\partial P_i/\partial[f\sigma_8]$.

This paper has been typeset from a TEX/LATEX file prepared by the author.